Available online at www.sciencedirect.com

SciVerse ScienceDirect

Ceramics International 39 (2013) S97–S102

CERAMICS INTERNATIONAL

www.elsevier.com/locate/ceramint

Enhanced piezoelectric properties of barium titanate–potassium niobate nano-structured ceramics by MPB engineering

Satoshi Wada[a,*], Kenta Yamashita[a], Ichiro Fujii[a], Kouichi Nakashima[a], Nobuhiro Kumada[a], Chikako Moriyoshi[b], Yoshihiro Kuroiwa[b]

[a]*Interdisciplinary Graduate School of Medical and Engineering, University of Yamanashi, Kofu, Yamanashi 400-8510, Japan*
[b]*Department of Physical Science, Hiroshima University, 1-3-1 Kagamiyama, Higashi-Hiroshima, Hiroshima 739-8526, Japan*

Available online 1 November 2012

Abstract

Barium titanate ($BaTiO_3$, BT)–potassium niobate ($KNbO_3$, KN) (BT–KN) nanocomplex ceramics with various KN/BT molar ratios were prepared by the solvothermal method. From a transmittance electron microscopy (TEM) observation, it was confirmed that KN layer thickness of the BT–KN nanocomplex ceramics was controlled from 0 to 44 nm by controlling KN/BT molar ratios. Their dielectric constants were measured at room temperature and 1 MHz, and a maximum dielectric constant of around 400 was measured for the BT–KN nanocomplex ceramics with a KN thickness of 22 nm. TEM observation revealed that below KN thickness of 22 nm, BT/KN heteroepitaxial interface was assigned to the strained interface while over 22 nm, the interface was assigned to the relaxed one. These results suggested that the strained heteroepitaxial interface could be responsible for the enhanced dielectric constants.

Keywords: Heteroepitaxial interface; Artificial MPB structure; Piezoelectric property

1. Introduction

Lead-free piezoelectric materials have been important in view of the environmental problems associated with conventional piezoelectrics of $Pb(Zr,Ti)O_3$ (PZT) ceramics [1]. However, the piezoelectric properties are lower than those of the PZT ceramics [2–4], and therefore it is difficult to replace them. Why do the PZT ceramics always show a high piezoelectric performance as compared to the lead-free ones? The high performance originates from a morphotropic phase boundary (MPB) structure. A transmittance electron microscopy (TEM) observation of a MPB composition of the PZT ceramics revealed very fine nano-ordered structures of three phases in one grain, i.e., the tetragonal phase, the rhombohedral phase, and the interface, while a synchrotron X-ray diffraction (XRD) measurement revealed the crystal structure of the MPB composition assigned to the monoclinic phase, which suggested that the origin of the monoclinic phase was a distorted interface region [5]. Moreover, the phenomenological approach [6] and the first principle calculation [7] proposed that the ultrahigh electromechanical response could be attributed to a polarization rotation mechanism (PRM) at the distorted interface region. Therefore, the MPB structure is the most important key to enhance the piezoelectric properties. For example, chemically modified KN and sodium niobate ($NaNbO_3$, NN) (KNN) ceramics have been reported as promising lead-free piezoelectrics with a new MPB, and their piezoelectric properties are similar to those of PZT ceramics [8,9]. However, it is not a universal microstructure, and systems with a MPB structure were limited. What can we do to create a MPB system? An artificial superlattice structure with a distorted interface region is one solution for this [10–12].

The MPB is, by definition, an epitaxial boundary between two thermodynamically stable ferroelectric phases in a phase diagram with temperature and chemical composition axes. In this study, MPB was extended to include an epitaxial boundary between two different ferroelectric

*Corresponding author.
E-mail address: swada@yamanashi.ac.jp (S. Wada).

0272-8842/$ - see front matter © 2012 Elsevier Ltd and Techna Group S.r.l. All rights reserved.
http://dx.doi.org/10.1016/j.ceramint.2012.10.042

materials that may create a solid solution if heated, e.g. the distorted interface of the artificial superlattice films, which was re-defined as an artificial MPB. For the artificial superlattice films, single crystal plates were used as substrates for an epitaxial film growth. If a single-crystal particle compact is used as a substrate for the epitaxial crystal growth, we can prepare complex nano-structured ceramics with the distorted interface region between the grown-crystal and the substrate particle compact, as shown in Fig. 1. Thus, if the distorted epitaxial interface region is created in the ceramics with a high density, we can design a variety of artificial MPB structures for piezoceramics.

Recently, barium titanate ($BaTiO_3$, BT) and strontium titanate ($SrTiO_3$, ST) (BT–ST) nanocomplex ceramics were successfully prepared by the solvothermal method, and it was reported that the interface was heteroepitaxial structure [13–15]. However, it was reported that their dielectric constants were below 100, and their strain behavior was poor. On the other hand, BT and potassium niobate ($KNbO_3$, KN) (BT–KN) nanocomplex ceramics were also prepared by the solvothermal method [16], and it was reported that the ceramics exhibited good ferroelectric property [17]. This is because BT has a tetragonal symmetry with a polar direction along [100], while KN has a monoclinic symmetry with a polar direction along [110], and their lattice mismatch is as small as 0.5% on the assumption that the system is a cubic cell [2,3]. Moreover, BT–KN system ceramics were reported as a unique ceramics system with the coexistence of the tetragonal and orthorhombic phases, and their dielectric and piezoelectric maxima were clearly observed in 0.5BT–0.5KN ceramics [18–22]. These results suggested that for BT–KN nanocomplex ceramics, the control of their microstructure, such as KN layer thickness, KN/BT interface density and connection between BT particles, could lead to enhancement of ferroelectric properties.

Thus, in this study, the BT–KN nanocomplex ceramics with various KN layer thickness were prepared by the solvothermal method, and their ferroelectric properties were measured. Finally, a relationship between KN layer thickness and ferroelectric properties was discussed.

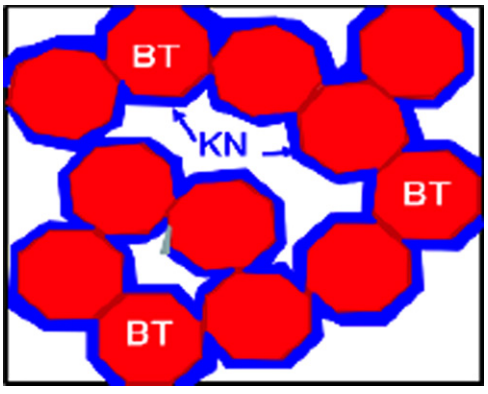

Fig. 1. Schematic image of the BT–KN nanocomplex ceramics with the artificial MPB structure and porosity of approximately 30%.

2. Experimental procedure

In this study, BT–KN nanocomplex ceramics were prepared by the solvothermal method with ethanol [16]. This is because water is harmful to BT owing to the easy elution of Ba ions from BT particles into water. Ethanol (EL grade, Kanto Chemical) was used as the solvent, while KOH (UGR grade, Kanto Chemical), K_2CO_3 (UGR grade, Kanto Chemical), Nb_2O_5 (99.9%, Kanto Chemical), and BT single-crystal particles (BTO_3, particle size of approximately 300 nm, Sakai Chemical Industry) were used as the starting materials. In this study, BTO_3 particles were selected as BT single-crystal particles with the shape of a polyhedron, because of the planar surfaces with crystallographic facets, suitable for epitaxial KN growth. The mixtures of BTO_3 and Nb_2O_5 powders with various KN/BT molar ratios from 0.1 to 1.0 were mixed with polyvinyl butyral (PVB, 2 wt%) as a binder in ethanol, dried at 130 °C, sieved, and then pressed into a green compact using a uniaxial press at room temperature. The binder was burned out at 600 °C for 10 h. Before the reaction, the density of the compact was measured by the Archimedes method with ethanol, and the crystal structure of the compact was investigated by conventional X-ray diffraction (XRD) analysis (Rigaku RINT2000, Cu Kα, 50 kV, 30 mA). The BTO_3 and Nb_2O_5 compact was placed in the Teflon-coated autoclave container with ethanol, KOH and K_2CO_3, heated up to temperatures below 230 °C, and soaked for 20 h without stirring. After the reaction, the compact was washed with ethanol and dried at 200 °C for 5 h. The density of the compact was measured by the Archimedes method with ethanol, and the crystal structure of the compact was investigated by XRD analysis. The microstructure was observed using scanning electron microscopy (SEM) and TEM. For electric measurements, the ceramics were polished and cut into a size of $2 \times 2 \times 0.5\ mm^3$. Gold electrodes were sputtered on the top and bottom surfaces with an area of $2 \times 2\ mm^2$. The dielectric properties were measured at various frequencies from 40 Hz to 10 MHz from 20 °C to 480 °C using an impedance analyzer (Agilent, HP4294A). The strain vs. electric-field (*S–E*) curves were measured at room temperature and 0.1 Hz using a ferroelectric character evaluation system, and a slope of the *S–E* curve was regarded as an apparent piezoelectric constant (d^*_{33}).

3. Results and discussion

3.1. Preparation of BT–KN nanocomplex ceramics with various KN/BT molar ratios

Using various KN/BT molar ratios from 0.1 to 1.0, BT–KN nanocomplex ceramics were prepared by the solvothermal method. Fig. 2 shows the KN/BT molar ratio dependence of relative density for the BT–KN nanocomplex ceramics before and after reaction. Relative densities of the compact before reaction were almost constant at around 60%, while after

reaction, the density of the BT–KN nanocomplex ceramics increased with increasing KN/BT molar ratios, and finally the maximum density of around 71% was obtained for the BT–KN nanocomplex ceramics with KN/BT molar ratio of 1.0. XRD measurement results revealed that after the reaction, XRD peaks associated with Nb_2O_5 almost disappeared and the formation of a large bridge structure between the tetragonal (002) and (200) BT peaks was clearly observed [16,17]. A similar "bridge structure" was reported for ferroelectric BT nanoparticles with three phases of a surface cubic phase, a bulk tetragonal phase, and the distorted interface region between the surface and the bulk [23], or BT fine-grained ceramics with a high density of 90° domain walls [24], and layered ST nanocubes epitaxially coated by BT [13]. The authors concluded that the "bridge structure" between the tetragonal (002) and (200) peaks could have originated from the distorted interface regions [13,17,23,24]. Thus, we believe that the observed "bridge structure" in this study can be attributed to distorted epitaxial KN growth layers on the BT particles. Moreover, a cross-sectional SEM observation of the reacted compact revealed that the KN crystal growth on BT surfaces resulted in a formation of strong connections between the BT particles with KN [17].

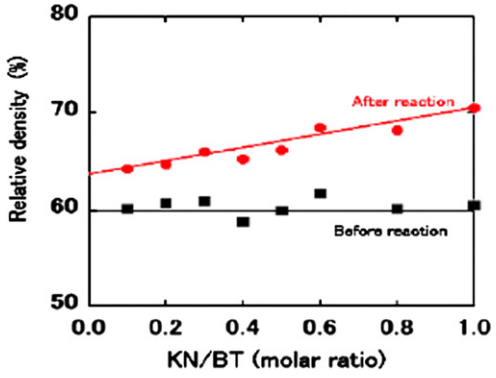

Fig. 2. KN/BT molar ratio dependence of relative density for the BT–KN nanocomplex ceramics before and after reaction.

Fig. 3 shows chemical composition distribution of Ba, Ti, O, K and Nb atoms for BT–KN nanocomplex ceramics with KN/BT molar ratio of 0.5. The distributions of Ba and Ti atoms were limited to the center of the complex particles, and their average diameter was estimated to be around 300 nm, which is almost consistent with the diameter of BTO_3 particles. On the other hand, the distributions of K and Nb atoms were limited to the shell region of the complex particles, and the average shell thickness was estimated to be around 24 nm. On the basis of Fig. 3, a simple model for the BT–KN complex particles was proposed, in which the particle was composed of two regions, i.e., BT core and KN shell, and the KN layer thickness was calculated for the BT–KN nanocomplex ceramics with various KN/BT molar ratios from 0 to 1.0 using the above model. Fig. 4 shows the KN/BT molar ratio dependence of the calculated KN layer thickness for the BT–KN nanocomplex ceramics. In addition, the measured KN average thickness from TEM observation was also plotted for the BT–KN nanocomplex ceramics with KN/BT molar ratios of 0.1, 0.2. 0.5 and 1.0. From Fig. 4, it is seen that the measured KN average thickness was almost consistent with the calculated ones. Moreover, their high resolution TEM images revealed that the ceramics had the heteroepitaxial interface between BT and KN [17]. The above discussion suggested that in this study, the BT–KN nanocomplex ceramics with various KN layer had average thickness from 5 to 40 nm.

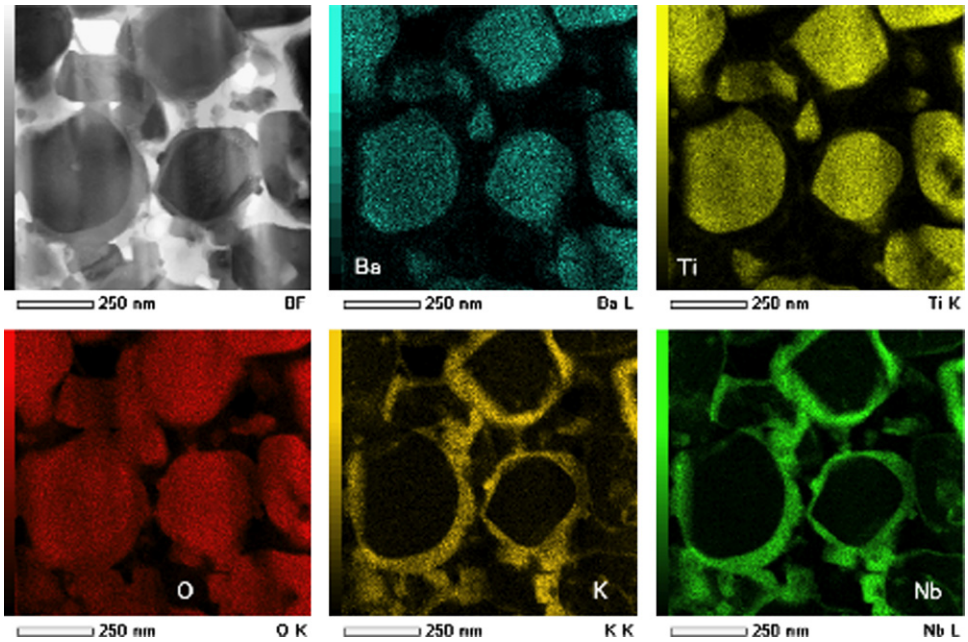

Fig. 3. Chemical composition distribution of BT–KN nanocomplex ceramics with KN/BT molar ratio of 0.5.

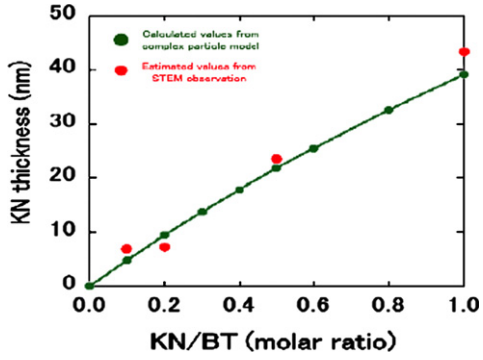

Fig. 4. KN/BT molar ratio dependence of KN layer thickness for the BT–KN nanocomplex ceramics.

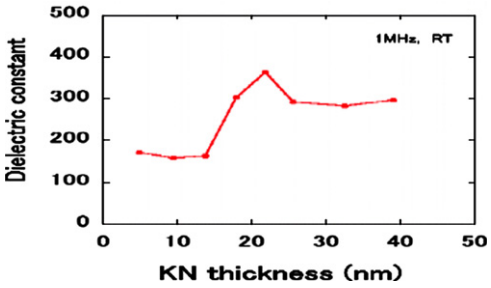

Fig. 5. KN layer thickness dependence of dielectric constants measured at room temperature and 1 MHz for the BT–KN nanocomplex ceramics.

3.2. Ferroelectric properties of BT–KN nanocomplex ceramics with various KN/BT molar ratios

The dielectric properties of the ceramics were measured at room temperature as a function of frequency from 40 Hz to 10 MHz. With increasing frequency, both the dielectric constant (ε_r) and loss tangent (tan δ) decreased gradually, and over 1 MHz, the ε_r and tan δ became almost constant [17]. Fig. 5 shows the KN layer thickness dependence of dielectric constants measured at room temperature and 1 MHz. It should be noted that for all of the BT–KN nanocomplex ceramics, loss tangent was below 5% at this measurement condition. From Fig. 5, below 15 nm, the dielectric constant was almost constant at 170, then at the KN thickness of 22 nm, the dielectric maximum of 370 was clearly observed. Above 22 nm, the dielectric constant was almost constant at around 300 despite KN thickness.

For KN porous ceramics with the porosity of around 30%, the ε_r was reported to be around 50 [25], while for the BTO_3 particle compact with the porosity of around 30%, the ε_r was reported to be around 62 [26]. As compared to the ε_r of 50 and 62 for each component, the ε_r of 370 of the porous BT–KN nanocomplex ceramics was much higher, which suggested that the interface region between BT and KN might contribute to the dielectric enhancement. However, we must explain why the dielectric constant exhibits the maximum at KN thickness of 22 nm. Thus, high resolution TEM observation was performed for the several BT–KN nanocomplex ceramics.

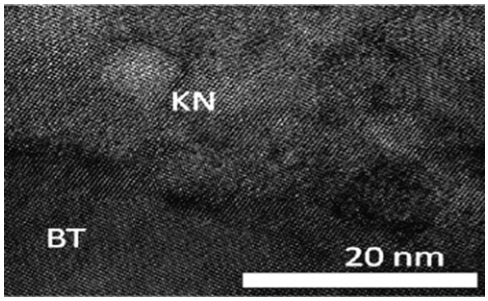

Fig. 6. High resolution TEM image of KN/BT interface for the BT–KN nanocomplex ceramics with KN/BT molar ratio of 0.5.

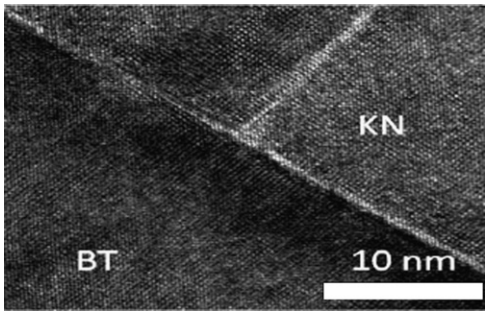

Fig. 7. High resolution TEM image of KN/BT interface for the BT–KN nanocomplex ceramics with KN/BT molar ratio of 1.0.

Fig. 6 shows a high resolution TEM image of KN/BT interface for the BT–KN nanocomplex ceramics with KN/BT molar ratio of 0.5 while Fig. 7 shows a high resolution TEM image of KN/BT interface for the BT–KN nanocomplex ceramics with KN/BT molar ratio of 1.0. Below KN thickness of 22 nm, there were no cracks and lattice mismatches at the KN/BT interface, which suggested that the KN/BT heteroepitaxial interface should be strained. On the other hand, at KN thickness of 40 nm, cracks and lattice mismatches accompanied with dislocations were partially observed, which suggested that the partial KN/BT heteroepitaxial interface should be relaxed.

We believe that if there are no cracks and no lattice mismatches at the KN/BT heteroepitaxial interface, the dielectric constant can increase with increasing KN layer thickness.

This is because the volume fraction of the distorted KN/BT interface should increase with increasing KN layer thickness if there are no cracks. For thin film application, it is well known that epitaxial film growth has thickness limitation, and this is one reason why KN/BT interface is relaxed over KN thickness of 22 nm.

Finally, the strain vs. electric field (*S–E*) and polarization vs. electric field (*P–E*) bipolar curves (Fig. 8) and the *S–E* unipolar curves (Fig. 9) were measured at room temperature for the BT–KN nanocomplex ceramics with various KN thickness. From Fig. 8, the *S–E* unipolar curve showed a typical ferroelectric butterfly-curve behavior, at KN/BT molar ratio of 0.8, the slope of the *S–E* curve became maximum, while at KN/BT molar ratio of

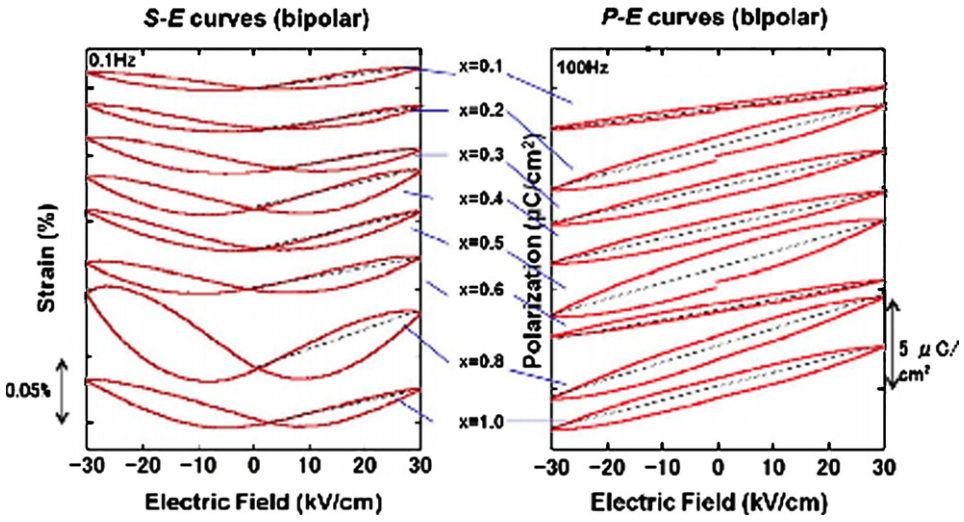

Fig. 8. KN/BT molar ratio dependences of *S–E* and *P–E* bipolar curves measured at room temperature for the BT–KN nanocomplex ceramics.

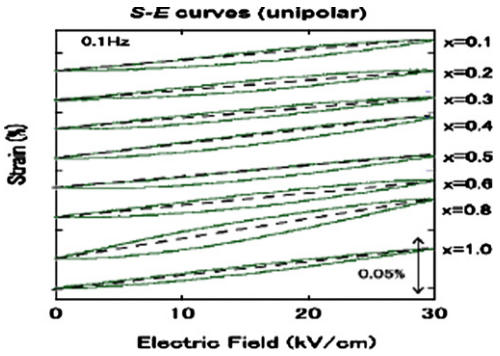

Fig. 9. KN/BT molar ratio dependence of *S–E* unipolar curves measured at room temperature and 0.1 Hz for the BT–KN nanocomplex ceramics.

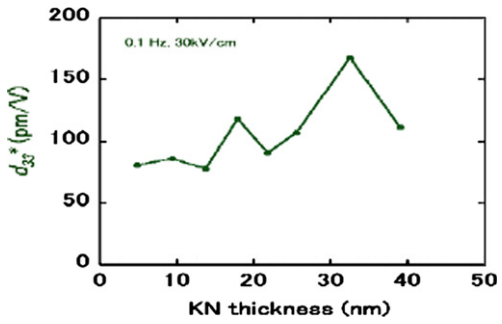

Fig. 10. KN layer thickness dependence of apparent piezoelectric constant d_{33}^* measured at room temperature and 0.1 Hz for the BT–KN nanocomplex ceramics.

0.5, the slope of the *P–E* curve became maximum, which suggested that the origin of strain behavior and dielectric behavior might be different.

From Fig. 9, the apparent piezoelectric constant d_{33}^* ($=S/E$) was estimated from a slope of the *S–E* unipolar curve. Fig. 10 shows KN layer thickness dependence of apparent piezoelectric constant d_{33}^* measured at room temperature and 0.1 Hz for the BT–KN nanocomplex ceramics. At a KN/BT molar ratio of 0.8, the apparent piezoelectric constant d_{33}^* was calculated to be 167 pC/N from a slope of the curve. Previously, for the 0.5BT–0.5KN dense ceramics with both the tetragonal and orthorhombic phases, the room temperature apparent d_{33}^* was reported to about 40 pC/N [18]. Therefore, the d_{33}^* value of 167 pC/N obtained in this study was four times larger than that of the 0.5BT–0.5KN dense ceramics [18], despite the BT–KN nanocomplex ceramics with the porosity of 30%. Thus, if the dense BT–KN nanocomplex ceramics were prepared, much higher d_{33}^* would be expected. Previously, the dielectric maximum was observed at KN thickness of 22 nm, and this may be caused by the distorted interface region between BT and KN. On the other hand, the piezoelectric maximum was observed at KN thickness of 33 nm, and this thickness is different between dielectric and piezoelectric properties. At present, we cannot explain the origin of the difference. However, piezoelectric properties are related to material softness in addition to dielectric properties, and are more complicated as compared to dielectric properties. To confirm this hypothesis, the interfaces for all of the BT–KN nanocomplex ceramics must be observed using high resolution TEM study.

4. Conclusions

In this study, the BT–KN nanocomplex ceramics with different KN layer thicknesses were prepared by the solvothermal method. From TEM observation, it was confirmed that KN layer thickness was controlled from 0 to 44 nm by controlling KN/BT molar ratios. Their dielectric constants were measured at room temperature and 1 MHz, and the maximum dielectric constant of 370 was measured at a KN thickness of 22 nm. A high resolution TEM observation revealed that below KN thickness of 22 nm, BT/KN heteroepitaxial interface was

assigned to strained interface while at 40 nm, the interface was assigned to the relaxed one. On the other hand, maximum apparent piezoelectric constant d^*_{33} was measured at a KN thickness of 33 nm. These results suggested that the strained heteroepitaxial interface could be responsible for the enhanced dielectric constants. However, the difference of KN layer thickness for dielectric and piezoelectric maximum cannot be explained now (because it is not known or because of the length of paper). We will explain the difference in the future on the basis of a more detailed interface structure.

Acknowledgments

The authors would like to thank Sakai Chemical Industry Co., Ltd. for providing the BTO_3 powders. The experiment at SPring-8 was carried out under Program nos. 2011A1667 and 2011B1732. This study was partially supported by the Elements Science and Technology Project from the Ministry of Education, Culture, Sports, Science and Technology, Japan (MEXT), and by a Grant-in-Aid for Scientific Research (No. 23656396) from MEXT.

References

[1] M. Demartin Maeder, D. Damjanovic, Piezoelectric Materials in Devices, N. Setter (Ed.), Lausanne, 2002.
[2] B. Jaffe, W.R. Cook Jr., H. Jaffe, in: Piezoelectric Ceramics, Academic Press, New York, 1971.
[3] F. Jona, G. Shirane, in: Ferroelectric Crystals, Dover, New York, 1993.
[4] Y. Zu, in: Ferroelectric Materials and Their Applications, North-Holland, Amsterdam, 1991.
[5] K.A. Schönau, L.A. Schmitt, M. Knapp, H. Fuess, R.-A. Eichel, H. Kungl, M.J. Hoffmann, Nanodomain structure of $Pb[Zr_{1-x}Ti_x]O_3$ at its morphotropic phase boundary: investigations from local to average structure, Physical Review B 75 (2007) 184117.
[6] Y. Ishibashi, M. Iwata, Morphotropic phase boundary in solid solution systems of perovskite-type oxide ferroelectrics, Japanese Journal of Applied Physics 37 (1998) L985–L987.
[7] H. Fu, R.E. Cohen, Polarization rotation mechanism for ultrahigh electromechanical response in single-crystal piezoelectrics, Nature 403 (2000) 281–283.
[8] Y. Saito, H. Takao, T. Tani, T. Nonoyama, K. Takatori, T. Homma, T. Nagata, M. Nakamura, Lead-free piezoceramics, Nature 432 (2004) 84–87.
[9] Y. Guo, K. Kakimoto, H. Ohsato, Phase transitional behavior and piezoelectric properties of $(Na_{0.5}K_{0.5})NbO_3$–$LiNbO_3$ ceramics, Applied Physics Letters 85 (2004) 4121–4123.
[10] T. Harigai, D. Tanaka, H. Kakemoto, S. Wada, T. Tsurumi, Dielectric properties of $BaTiO_3/SrTiO_3$ superlattices measured with interdigital electrodes and electromagnetic field analysis, Journal of Applied Physics 94 (2003) 7923–7925.
[11] A.Q. Jiang, J.F. Scott, H. Lu, Z. Chen, Phase transitions and polarizations in epitaxial $BaTiO_3/SrTiO_3$ superlattices studied by second-harmonic generation, Journal of Applied Physics 93 (2003) 1180–1185.
[12] K. Johnston, X. Huang, J.B. Neaton, K.M. Rabe, First-principles study of symmetry lowering and polarization in $BaTiO_3/SrTiO_3$ superlattices with in-plane expansion, Physical Review B 71 (2005) 100103.
[13] T. Goto, K. Nakashima, I. Fujii, Y. Kuroiwa, Y. Makita, S. Wada, Preparation of barium titanate/strontium titanate multilayered nanoparticles, Key Engineering Materials 485 (2011) 305–308.
[14] S. Iwatsuki, T. Goto, M. Kera, K. Nakashima, I. Fujii, S. Wada, Preparation of barium titanate-coated strontium titanate accumulation ceramics by solvothermal synthesis and their dielectric property, Key Engineering Materials (in press).
[15] T. Goto, S. Iwatsuki, M. Kera, K. Nakashima, I. Fujii, S. Wada, Preparation of strontium titanate-coated barium titanate accumulation ceramics by solvothermal synthesis and their dielectric property, Key Engineering Materials (in press).
[16] S. Wada, S. Shimizu, K. Yamashita, I. Fujii, K. Nakashima, N. Kumada, Y. Kuroiwa, Y. Fujikawa, D. Tanaka, M. Furukawa, Preparation of barium titanate–potassium niobate nanostructured ceramics with artificial morphotropic phase boundary structure by solvothermal method, Japanese Journal of Applied Physics 50 (2011) 09NC08.
[17] I. Fujii, S. Shimizu, K. Yamashita, K. Nakashima, N. Kumada, C. Moriyoshi, Y. Kuroiwa, Y. Fujikawa, D. Tanaka, M. Furukawa, S. Wada, Enhanced piezoelectric response of $BaTiO_3$–$KNbO_3$ composites, Applied Physics Letters 99 (2011) 202902.
[18] S. Wada, M. Nitta, N. Kumada, D. Tanaka, M. Furukawa, S. Ohno, C. Moriyoshi, Y. Kuroiwa, Preparation of barium titanate–potassium niobate solid solution system ceramics and their piezoelectric properties, Japanese Journal of Applied Physics 47 (2008) 7678–7684.
[19] S. Wada, M. Nitta, N. Kumada, D. Tanaka, M. Furukawa, C. Moriyoshi, Y. Kuroiwa, Phase diagram and microstructure analysis of barium titanate–potassium niobate system piezoelectric ceramics, Key Engineering Materials 421–422 (2010) 34–37.
[20] S. Wada, S. Shimizu, P. Pulpan, N. Kumada, D. Tanaka, M. Furukawa, C. Moriyoshi, Y. Kuroiwa, Preparation of barium titanate–potassium niobate ceramics using interface engineering and their piezoelectric properties, Journal of the Ceramic Society of Japan 118 (2010) 691–695.
[21] S. Shimizu, P. Pulpan, N. Kumada, D. Tanaka, M. Furukawa, Y. Kuroiwa, T. Suzuki, T. Uchikoshi, S. Wada, Enhanced piezoelectric properties of barium titanate–potassium niobate solid solution system ceramics by MPB engineering, Key Engineering Materials 445 (2010) 11–14.
[22] S. Shimizu, N. Kumada, K. Nakashima, I. Fujii, D. Tanaka, M. Furukawa, Y. Kuroiwa, T. Suzuki, T. Uchikoshi, Y. Sakka, S. Wada, Microstructure control of barium titanate–potassium niobate solid solution system ceramics by MPB engineering and their piezoelectric properties, Key Engineering Materials 485 (2011) 89–92.
[23] T. Hoshina, S. Wada, Y. Kuroiwa, T. Tsurumi, Composite structure and size effect of barium titanate nanoparticles, Applied Physics Letters 93 (2008) 192914.
[24] T. Hoshina, K. Takizawa, J. Li, T. Kasama, H. Kakemoto, T. Tsurumi, Domain size effect on dielectric properties of barium titanate ceramics, Japanese Journal of Applied Physics 47 (2008) 7607–7611.
[25] S. Wada, Y. Mase, S. Shimizu, K. Maeda, I. Fujii, K. Nakashima, P. Pulpan, N. Miyajima, Piezoelectric properties of porous potassium niobate system ceramics, Key Engineering Materials 485 (2011) 61–64.
[26] A. Yazawa, T. Hoshina, H. Kakemoto, T. Tsurumi, S. Wada, Preparation and dielectric properties of 3D barium titanate colloidal sphere array, Key Engineering Materials 320 (2006) 127–130.